Performance of a Solar Hot Water System

Bob Tingleff

May 3, 2007

Abstract

A model of a solar hot water heating system is developed based on hourly radiation data. The model is used to simulate an installation in Santa Cruz, California. Alternative configuration options at the site are investigated. Tilt and orientation of the collector surface are varied to determine the optimal values. The fraction of annual water heating is determined for various configurations of the solar energy system, and the economic benefits are compared. The configurations examined provided more than 60% of the annual hot water. No system was found to be as cost-effective as a 70% efficient natural gas fueled water heater.

Contents

1 Introduction **1**

2 Literature Review **2**

2.1 Solar radiation 2

2.2 Solar collectors 3

2.3 Additional system components 5

2.4 Simulations 6

2.5 System sizing 7

3 Methodology **7**

3.1 Solar radiation 8

3.2 Solar collector 10

3.3 Heat transfer to storage 12

3.4 Flow rate correction 15

4 Model application **15**

4.1 Collector model 16

4.2 Tank and heat exchanger 16

4.3 Flow rate 17

4.4 Fraction of DHW supplied 17

4.5 Economic analysis 18

4.6 Model uncertainty 18

5 Results and discussion **19**

5.1 Model validation 19

5.2 Model output 20

5.3 Collector tilt and orientation 21

5.4 Collector area 23

5.5 Flow rate 24

5.6 Economic analysis 25

6 Conclusions **26**

1 Introduction

This study meets the requirements of a requested analysis of a solar water heating system. The requirements called for a model and analysis capable of providing basic design parameters such as the sizing, orientation and other basic elements of the solar water heating system. The model described herein proposes a method of providing these parameters.

Worldwide, the most common use of solar energy is the provision of domestic hot water (DHW) (I.E.A., 2004). A number of design issues arise with any solar DHW application, including type of collector, size of collector, storage size, collector orientation, and others. System parameters are chosen to meet specified design goals, such as providing a certain fraction of the heating load, or meeting the optimum life-cycle cost of heating energy.

This study investigates a specific solar DHW system at a residence in Santa Cruz, California, by developing a model of the system. The collector is oriented due South, at a tilt of 18°, with no shading. The study seeks to determine the fraction of the annual heating load met by various system configurations, with the goal of characterizing and optimizing the life-cycle cost/benefit relationship. In addition, other parameters of the system, such as collector tilt and orientation, are investigated. The current system consists of one 4ft.×10ft. collector, and an 80-gallon storage tank. The study will determine whether a 4ft.×8ft. collector would be more cost-effective, the cost effectiveness of purchasing an additional collector, and the benefits of using a higher quality collector.

2 Literature Review

2.1 Solar radiation

Solar radiation is an important factor in any solar energy system model. The solar radiation striking a surface on the earth depends on the time of year, time of day, tilt of the surface from horizontal, and compass orientation, or azimuth, of the surface (Bush and Richards, 1980). Based on spherical geometry, equations relate the solar radiation striking a collector to the latitude at the site, the collector's tilt and orientation, and the solar time.

In the 1970's in the United States, a program of collecting solar radiation data was extended to many cities across the country, producing the National Solar Radiation Data Base (NSRDB) (Maxwell, 1998). At some sites, measurements were made of total radiation striking a horizontal surface; at other locations additional measurements were made of the diffuse (non-beam) radiation striking the surface. However, most of the entries in the NSRDB are generated from the Meteorological/Statistical (METSTAT) model, rather than radiation measurements. The model incorporates hourly water vapor and cloud cover data, surface albedo conditions, and solar geometry to generate hourly solar direct and diffuse radiation values. Marion and George (2001) incorporated surface weather observations of cloud cover from weather stations around the world into the METSTAT model, generating modeled solar data for sites worldwide.

Because cloud cover information is frequently recorded in weather data, a number of models have attempted to produce solar radiation values based on solar geometry and cloud cover data (Muneer and Gul, 2000). Additional parameters include aerosol concentration, and concentrations of various gases, including $CO_2, NO_2, \text{and} O_3$ (Gueymard, 2003).

2.2 Solar collectors

Solar collectors can be categorized as batch, flat-plate, concentrating, and evacuated-tube (Kalogirou, 2004). The most common type used in the United States is the flat-plate collector (Weiss et al., 2005). The most common collector configuration consists of parallel riser tubes, which carry the heat-transfer fluid, attached to manifolds at the top and bottom of the collector (Figure 2.1). The tube carrying the fluid may be a single serpentine tube rather than a series of parallel tubes. Fins, which are the energy-absorbing surfaces, are bonded to the riser tubes. The tube and fin structure is insulated underneath and on the sides, and is typically covered with one or more layers of a transparent glazing, such as glass.

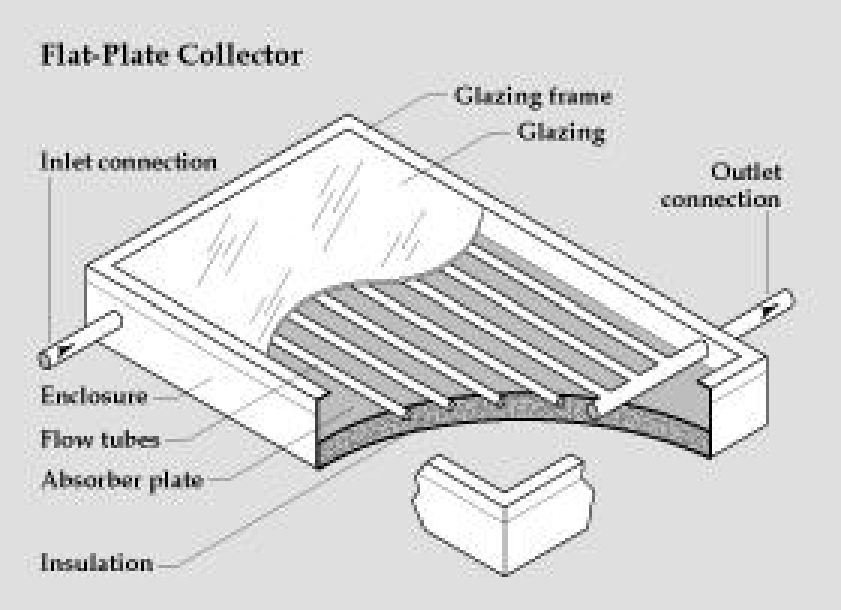

Fig. 2.1: The basic elements of a typical flat plate collector are shown (DOE, 2006).

Energy balance equations form the basis of models of solar thermal collectors. Flat-plate collectors have been modeled with varying degrees of complexity. Kazeminejad (2002) compared one and two-dimensional steady-state models of the conduction equations for the fins and tubes of the collector. The equations model the temperature distribution in the ab-

sorber surface, the conduction through the tube to the fluid, and the overall loss through the glazing. The equations were solved with a finite difference method. Empirical relations were used for the overall loss coefficients. Kalogirou (2004) modeled the collector surface as a classical steady-state fin problem. The temperature distribution in the fin is considered to be constant along the length of the collector.

Petkovsek and Rakovec (1983) modeled a flat-plate collector with two energy balance equations, one for the glazing and one for the collector. A total of 17 energy flux terms were used in the system of equations, including radiation, conduction, and convection terms for each system component, and terms for the effects of ambient temperature, humidity, wind speed, and insolation. Most models make use of simplifying assumptions. Conceptually, the radiative losses are based on the differences between the fourth powers of the collector and background temperatures, and the convective losses are extremely complex. However, convection and radiative losses from the top plate of the collector are often modeled together as a simple linear relationship with wind speed (Duffie and Beckman, 2006). Onur (1993) experimentally investigated the accuracy of the linear model using scale model collectors. Using a variety of wind speeds and directions, differences of up to 15% between the more complex and the simplified models were reported.

In addition to the simplifying assumption of linear radiative losses, additional assumptions of average collector plate temperature, average convective heat transfer coefficient, and steady-state conditions are often made (Kalogirou, 2004); the resultant model contains a collector efficiency factor and relates the efficiency of energy collection to that which would occur with no losses. This model is used to rate solar collectors (Duffie and Beckman, 2006). The transient form of the model is used as the basis for measuring a collector's "time constant," which reflects the energy stored in the thermal mass of the collector (Hou et al., 2005).

2.3 Additional system components

Other important elements of a solar DHW system potentially include a pump, a storage tank, pipes, and a heat exchanger. The pump is not directly part of the energy balance, but the flow rate is important in the collector equations. The tank can be modeled as lumped storage (Badescu and Staicovici, 2006), a plug-flow reactor (Kleinbach et al., 1993), or using more detailed computational fluid dynamic (CFD) models. Thermal stratification in the tank is important to overall system performance because the hot water at the top of the tank is closer to the temperature demanded, and the colder water at the bottom enables higher efficiencies in the collector (Li and Sumathy, 2002). Oliveski et al. (2003) compared one and two-dimensional models of storage tanks based on conservation of mass, energy, and momentum. The one-dimensional models produce impossible results at the boundaries, requiring computational artifices. However, these models produce temperature results very similar to experimental data.

Kleinbach et al. (1993) compared a plug-flow model with a multi-node "plume entrainment" model, which models incoming water as a momentum-driven jet. Finite volume methods were used to solve the equations. Heat can be transferred to the storage tank directly with the mass of water injected into the tank after passing through the collector, or indirectly through a heat exchanger. A tube and fin coil can be inserted directly into the storage tank, or the tank can be surrounded by an insulated "mantle" heat exchanger. Badescu and Staicovici (2006) modeled the performance of an immersed coil by breaking the coil into discrete sections, each with its own local heat transfer coefficient between heat transfer fluid and coil walls, and between coil walls and water in the tank. Standard algebraic equations for convective heat transfer can then be solved. Marshall (1999) found that a heat exchanger effectiveness greater than 0.5 has little effect on system performance, and used this static value in models of solar DHW systems. He also found that pipe losses, commonly ignored,

are more important than usually assumed.

2.4 Simulations

Models of solar DHW systems are implemented as computer simulations. A number of packages exist that incorporate the DHW systems into whole-house models (Badescu and Staicovici, 2006). TRNSYS is one such model, and has modules for house loads, passive space heating, and active solar elements including pump, collector, heat exchanger, and storage (Duffie and Beckman, 2006). Pillai and Banerjee (2007) used TRNSYS to evaluate the fraction of water heating that could be economically met with solar energy for a hypothetical area in India. Assumptions were made that load patterns and solar energy system performance were typical. Economies of scale were crucial; they found that only 4% of the load in single-family homes would be met economically, but that 65% of hotel demand could be economically met with solar systems. Biaou and Bernier (2007) used TRNSYS to model solar hot water systems in Los Angeles and Montreal. They found that a solar collector area of 4.5 m^2 would be required to meet 100% of the hot water requirements of a residence in Los Angeles. TRNSYS was used together with a linear programming optimization program, OPTLIB, to find the optimal economic size for a collector in Sao Paulo, Brazil(Lima et al., 2006). The optimal size economically provided up to 38% of the annual heating. This was far less than the maximum fraction provided by solar energy among the options they considered, which was over 90%.

A simulation of a "passive solar house" in Germany, using a program written specifically for the house, found that the DHW energy demand was about 70% of the heating load (Badescu, 2005). The fraction met by the solar collectors varied from 25% to 93%, with an annual average of 60%. Bojic et al. (2002) investigated a solar DHW system at a four-person household in Yugoslavia using a custom-developed "time marching" simulation program.

Two profiles of hot water consumption were used – a static profile, and a more realistic profile which varied throughout the day. The results indicated that larger storage tank size led to the solar system meeting a larger fraction of the heating load.

2.5 System sizing

In practice, solar DHW systems are generally sized using "rules of thumb." For example, contractors often recommend 20 square feet of collector for the first two people in a house, and 8 to 14 additional square feet for each additional occupant, depending on the climate (DOE, 2007). The National Renewable Energy Laboratory (NREL) recommends that a system be sized to meet 90–100% of the summer load (NREL, 2007). To qualify for federal tax credits, a system must meet at least 50% of the household's annual DHW needs (Bickford, 2007).

The demand for hot water in a household is generally estimated by typical reported usage values, although detailed surveys can be made. Estimates of household usage range from 15 gallons per person per day for an efficient household (Bickford, 2007) to 40 gallons per person per day for an average household (NREL, 2007). The collector area can be sized by dividing the average daily usage by the product of the average collector efficiency (typically around 40%) and the average daily insolation.

3 Methodology

Hourly values for solar radiation on a horizontal surface are available from the NSRDB for the San Francisco Airport for the years 1961–1990 (NSRDB, 2007). Modeled radiation estimates are provided for total, direct, and diffuse radiation. Values are flagged with estimates of the uncertainty; typical estimates of uncertainty are under 10%. NREL provides a Typical Meteorological Year (TMY) summary, which is intended for use in simulations. The TMY

data set includes values from selected months from the 30-year period. The months selected were chosen as those which most closely matched the 30-year average values for the month in a number of categories, including radiation, temperature, and wind speed (Marion and Urban, 1995). The airport site is the closest available to the location in this study, and has a similar climate to that in Santa Cruz.

3.1 Solar radiation

The model used here is based on the development in Duffie and Beckman (2006). The radiation falling on the collector is derived from the data as follows. The radiation on a tilted surface for an hour is the sum of the direct, diffuse, and ground reflected radiation,

$$I_T = I_b R_b + I_d(\frac{1+cos\beta}{2}) + I\rho_g(\frac{1-cos\beta}{2}) \tag{1}$$

where

I_T	is	the hourly radiation on the tilted surface (W-hrs or J)
I_b	is	the direct beam component of solar radiation on a horizontal surface (J)
I_d	is	the diffuse component of the radiation on a horizontal surface (J)
R_b	is	the ratio of beam radiation on a tilted surface to that on a horizontal surface
ρ_g	is	a ground reflectance coefficient
β	is	the tilt angle of the collector (°)

The radiation values $I, I_b,$ andI_d are provided in the modeled data for the site. The ratio R_b is determined from,

$$R_b = \frac{cos\theta}{cos\theta_z} \tag{2}$$

where

θ is the angle between a normal to the collector surface and a line from the surface to the sun (°)

θ_z is the solar zenith angle, or the angle between the vertical and a line from the earth's surface to the sun (°)

The angle θ is determined from,

$$\begin{aligned} cos\theta &= sin\delta sin\phi cos\beta - sin\delta cos\phi sin\beta cos\gamma + cos\delta cos\phi cos\beta cos\omega \\ &\quad + cos\delta sin\phi sin\beta cos\gamma cos\omega + cos\delta sin\beta sin\gamma sin\omega \end{aligned}$$

where

δ is the earth's declination with the sun (°)

ϕ is the site's latitude (°)

γ is the collector azimuth (°)

ω is the hour angle (°)

The declination, δ, varies seasonally, with zero values at the equinoxes, according to the formula,

$$\delta = 23.45 sin(360 \frac{284 + n}{365}) \tag{3}$$

where n is the day of the year.

The hour angle ω is defined as zero at solar noon, and varies by $\pm 15°$ per hour away from solar noon. To calculate the hour angle, solar time is needed, and is related to standard time by,

$$SolarTime = StandardTime + 4(L_{st} - L_{loc}) + E \tag{4}$$

where

L_{st} is the standard meridian for the site (°)

L_{loc} is the actual meridian at the site (°)

E is known as the equation of time (minutes)

The equation of time value represents the perturbations in the earth's rate of rotation, and is derived from,

$$E = 229.2(0.000075 + 0.001868cosB - 0.032077sinB - 0.0141615cos2B - 0.04089sin2B) \quad (5)$$

where B is defined as

$$B = (n-1)\frac{360}{365} \quad (6)$$

The solar azimuth angle, θ_z is derived from,

$$cos\theta_z = cos\phi cos\delta cos\omega + cos\phi sin\delta \quad (7)$$

These equations, combined with the hourly radiation data on a horizontal surface, are sufficient to estimate the radiation impinging on the collector surface on an hourly basis.

3.2 Solar collector

The model for the collector is based on the equation (Duffie and Beckman, 2006),

$$\dot{Q}_u = A_c[S - U_L(T_{pm} - T_a)] \quad (8)$$

where where

$\dot{Q}_u$ is the rate of heat transferred to the collector fluid (W/m^2)

A_c is the collector area (m^2)

S is the hourly radiation absorbed by the collector surface ($kWh/h\ m^2$)

U_L is the overall collector heat loss coefficient (W/m^2K)

T_{pm} is the average collector plate temperature ($^\circ C$)

T_a is the ambient temperature ($^\circ C$)

A multiplier is needed to convert the hourly term to Watts. The model has two terms: energy absorbed and energy lost. Losses are proportional to the difference between collector temperature and ambient temperature. The overall loss coefficient varies with conditions, especially wind speed. Plate temperature is difficult to know; the water inlet temperature can be substituted if a collector heat removal factor F_R is added to the equation,

$$\dot{Q}_u = A_c F_R[S - U_L(T_i - T_a)] \tag{9}$$

The absorbed radiation S is derived from the solar input expressions described above, with the addition of an optical transmittance component,

$$S = I_b R_b(\tau\alpha)_b + I_d(\tau\alpha)_d(\frac{1+cos\beta}{2}) + I\rho_g(\tau\alpha)_g(\frac{1-cos\beta}{2}) \tag{10}$$

The $(\tau\alpha)$ terms include the losses due to reflection and absorption in the glazing, and are a function of angle of incidence of the radiation. The beam component of the optical transmittance can be expressed,

$$(\tau\alpha)_b = k_{\tau\alpha,b}(\tau\alpha)_n \tag{11}$$

where

$(\tau\alpha)_n$ is the fraction of normal beam radiation transmitted

$k_{\tau\alpha,b}$ is $1 - b_0(\frac{1}{cos\theta} - 1)$

The diffuse and ground optical transmittance terms are defined similarly, except that the angle θ is not the incidence angle. It is determined by consulting tables that provide θ as a constant angle function of collector tilt angle.

Equations 9, 10, and 11 can be combined into the collector efficiency equation,

$$\eta = \frac{\dot{Q}_u}{SA_c} = F_R(\tau\alpha)_n - F_R U_L(\frac{T_i - T_a}{S}) \tag{12}$$

The quantities $F_R(\tau\alpha)_n$ and $F_R U_L$ are constant collector parameters, and are the intercept and slope of this linear equation. These parameters are determined in standardized collector testing procedures. If the collector is actually used in windy conditions, the loss parameter ($F_R U_L$) will have a systematic bias that underestimates the losses, since the testing is carried out under low wind-speed conditions.

3.3 Heat transfer to storage

The energy transferred by the heat transfer fluid (water in this case) is transferred to the storage tank through the heat exchanger. A constant heat exchanger effectiveness of 0.6 is assumed. The tank is modeled as fully mixed. The temperature change in the collector fluid is determined from,

$$Q_u = m_f C_p \Delta T_f \tag{13}$$

where

m_f is the mass of fluid passing through the collector during one time period (kg)

C_p is the specific heat capacity of water ($J/kg\ K$)

ΔT_f is the temperature change of the collector fluid ($^\circ C$)

The temperature change in the tank water is modeled with the heat exchanger effectiveness equation,

$$m_T C_p \Delta T_T = \epsilon m_f C_p (T_f - T_{T1}) \tag{14}$$

where ΔT_T is the temperature change in tank water temperature, and T_{T1} is the starting tank temperature.

The flow rate, $\dot{m}$, is determined by the pump and the head. The pump manufacturer provides a curve relating flow to head. For the pump speed used, this is a linear relationship. The head is a combination of static head, which is measured, and the friction losses in the pipes. The pipe lengths include the collector supply and return, the riser tubes, and the heat exchanger. The flow rate can be determined through an iterative root-finding procedure as follows. The head loss in a pipe can be estimated from the Darcy-Weisbach equation (Crowe et al., 2005).

$$h_f = f \frac{LV^2}{D2g} \tag{15}$$

where

h_f is the friction loss ($ft.$)

f is a friction factor

L is the length of pipe ($ft.$)

V is the average fluid velocity ($ft./sec$)

D is the pipe diameter ($ft.$)

g is gravitational acceleration ($ft./sec^2$)

The head loss is therefore a function of the fluid velocity, or flow rate. The friction factor can be found from the Colebrook equation,

$$\frac{1}{\sqrt{f}} = -2log(\frac{\epsilon/D}{3.7} + \frac{2.51}{Re\sqrt{f}}) \tag{16}$$

where

ϵ is the smoothness coefficient of the pipe ($ft.$)

Re is the Reynolds number for the flow

The Reynolds number for pipe flow is defined as,

$$Re = \frac{VD}{\nu} \tag{17}$$

where ν is the kinematic viscosity of water.

The Colebrook equation cannot be solved explicitly for f; an iterative procedure must be used. The procedure is initiated with an estimate of the flow. The Darcy-Weisbach equation is solved for f, and this expression is substituted into the Colebrook equation, which is solved for f using the secant root-finding method. This value of f yields a value for h_f. This procedure is carried out for each section of pipe. The smoothness coefficients for the heat exchanger can be estimated from its length, diameter, and the manufacturer's specification of head loss at a known flow rate.

The final step in the procedure is to compare (head loss,flow) pairs of values with the curve provided by the pump manufacturer for the best fit. The problem is over-determined; the fit is not expected to be perfect.

3.4 Flow rate correction

The flow rate used in the testing procedure is reported along with the collector parameters. When the collector is operated at a different flow rate, a correction ratio, r, is applied to the collector parameters:

$$r = \frac{F_R U_L|_{use}}{F_R U_L|_{test}} = \frac{F_R(\tau\alpha)_n|_{use}}{F_R(\tau\alpha)_n|_{test}} \tag{18}$$

The ratio r is found from

$$r = \frac{\frac{\dot{m}C_p}{A_c F' U_L}[1 - exp(-A_c F' U_L/\dot{m}C_p)]|_{use}}{F_R U_L|_{test}} \tag{19}$$

where $F'U_L$ is determined from,

$$F'U_L = -\frac{\dot{m}C_p}{A_c} ln(1 - \frac{F_R U_L A_c}{\dot{m}C_p}) \tag{20}$$

4 Model application

A FORTRAN program (Appendix A) was written to simulate the solar DHW system. The model for the collector is based on Equation 9, and uses TMY hourly radiation data for the San Francisco Airport. Model parameters tilt and orientation were varied to determine the optimum siting characteristics. Five collector configurations, using two different collector surfaces, were modeled to determine the fraction of annual DHW provided. Finally, the economic value of the solar DHW system's configurations were compared with each other, and with an all-natural gas system.

4.1 Collector model

The useful energy captured in the collector fluid (water in this case) is described by Equations 9, 10, and 11. Standard testing procedures determine the parameters $F_R(\tau\alpha)_n, F_R U_L$, and b_0 (Duffie and Beckman, 2006). The collectors examined are manufactured by Radco Solar, Inc. (Table 4.1). Two collector surfaces are available: black paint, and a chrome, "selective surface," which has a low radiative emissivity in infrared wavelengths, and thus lower losses. Standard sizes are 32 and 40 square feet.

Table 4.1: Radco Solar collectors are available in two sizes, and with a painted or selective surface (a: (SRCC, 2007); b:(Solarskies, 2007))

Collector	Dimensions	$F_R(\tau\alpha)_n$ [a]	$F_R U_L$ [a]	b_0 [a]	Surface	Cost [b]
408P-HP	4ft.×8ft.	0.768	-7.24	-0.123	Black paint	$858
410P-HP	4ft.×10ft.	0.768	-7.24	-0.123	Black paint	$1045
408C-HP	4ft.×8ft.	0.779	-4.77	-0.123	Black chrome	$1048
410C-HP	4ft.×10ft.	0.779	-4.77	-0.123	Black chrome	$1418

4.2 Tank and heat exchanger

In actual operation, a controller switches on the pump based on the temperature difference between the tank water and the collector surface. To model this in the simulation, if the incoming radiation is less than a minimum value, it is discarded. The tank was modeled as completely mixed. The temperature change in the collector fluid, an important model variable, is described by Equation 13, and the temperature change in the tank is described by Equation 14. Incoming cold water was specified as 11°C. The demand for hot water was modeled as a single event, occurring between 8:00PM and 9:00PM. The base daily hot water demand assumed was 150 liters.

4.3 Flow rate

The pump manufacturer provides a curve describing flow rate as a function of head. For the pump and speed used, this curve is the linear model, $q = 10.1 - h$. The head is the sum of the static head, 6 feet, and the friction losses in the supply pipes (56 feet, 3/4 inch diameter), the heat exchanger (30 feet, 1 inch diameter), and the collector riser tubes (122 feet, 3/8 inch diameter). The smoothness coefficient ϵ used for the pipes and risers was that for smooth pipes, 6×10^{-5} inches (Crowe et al., 2005). The smoothness coefficient for the heat exchanger was found by solving Equation 15 for the friction factor, based on the manufacturer's specification of 9.1 feet head loss at 12 gpm, and then explicitly solving Equation 16 for ϵ. Each section of pipe was then solved iteratively using the Secant Method (Appendix A) for h_f as a function of flow rate. Finally, the (flow, head loss) pair was compared with the manufacturer's curve. The pair with the least geometric distance to the curve was (1.7gpm, 8.41 ft.), with a distance of 0.0053 to the curve.

4.4 Fraction of DHW supplied

The daily energy supplied by the solar DHW system is calculated as the sum of hourly energy quantities supplied to the tank (Equation 14). The energy supplied to the household is limited by the quantity that can be transferred in the volume of water demanded at the temperature of the tank water at the time of the demand, according to Equation 14. The demand is modeled as the energy required to heat 150 liters per day from 11°C (52°F) to 49°C (120°F) per day. The model reports the annual fraction of DHW provided by the solar DHW system.

4.5 Economic analysis

The present values for a 25-year life span of system configurations were compared with each other and with the present value of heating the water with a natural gas heater (assumed 70% efficient). Natural gas costs were described as an escalating uniform series (Sandia_National_Laboratory, 2002), with an initial gas cost of $1.24 per therm (PG&E, 2007), a discount rate of 5%, and an escalation rate of 2%. The present value of the solar DHW system includes capital and installation costs, as well as assumed periodic maintenance costs equal to 3% of the initial costs every five years. Configurations examined were one or two collectors, either of which could be 4 ft.×8 ft. or 4 ft.×10 ft. (allowing five possible configurations). Each of the five area options was modeled with each collector surface option. The energy escalation rate was varied in a sensitivity analysis. Initial costs other than collector costs include the cost of the tank, balance of system components, and installation costs (Table 4.2). The larger storage tank was used with the two-collector configurations.

Table 4.2: Initial costs in addition to the collector bring the minimum cost of the system to over $5000 (a: (RadiantHeatProducts, 2007)).

Item	Cost
Superstor 80 gal tank[a]	$1575
Superstor 120 gal tank[a]	$2125
Pump, controller, pipes, drainback tank, etc.	$500
Installation, with one collector	$2380
Installation, with two collectors	$2880

4.6 Model uncertainty

Sources of error in the model include:

- the assumption of constant radiation and temperature during the one-hour time step

of the simulation

- errors in the METSTAT radiation model
- differences between Santa Cruz and San Francisco Airport radiation and temperatures
- the assumption of no losses from the tank and pipes
- inaccuracies in the DHW demand profile
- differences in the Santa Cruz environment and that assumed in the collector loss coefficient

In addition, actual years will differ from the TMY used in this model.

5 Results and discussion

5.1 Model validation

The model has not been calibrated against actual data. However, several results indicate that the model portrays the physical situation reasonably well. The annual average daily energy collected and transferred to the storage tank according to the model, 35MJ, is within the range of 26-40MJ specified by SRCC for this collector for cloudy to clear conditions. The "f-chart method" (Duffie and Beckman, 2006) was also used to estimate the annual fraction of water heating provided by the solar collector. This method is based on monthly average radiation and temperature values, as well as collector parameters. It is considered to be accurate to within 10-15% (Duffie and Beckman, 2006). The FORTRAN model developed here predicted that 66% of the water heating load would be met in the base case by solar energy; the f-chart prediction was 77%. In addition, examination of the temperature values

developed in the model matches casual observation of the system. Storage tank temperatures reach 150°F on a few days of the year. During the summer, tank temperatures often exceed 120°F. In the winter, tank temperatures at the end of the day range from 80-100°F.

A shortcoming of the model is that losses from the tank and pipes are not incorporated. This is noticeably different from the actual situation - in the model the tank water temperature remains the same overnight; in reality it drops. On the other hand, the model ignores thermal stratification in the tank, which leads to underestimating the energy supplied. In addition, the hot water demand in the model occurs at one moment in the evening. A more realistic model would incorporate stochastic demand based on surveys of actual households.

5.2 Model output

The main state variable in the model is the tank water temperature. During a week in May, the tank temperature rises according to the radiation input (Figure 5.2). The week begins with a cloudy day, and ends with a completely sunny day. The limitations of the model can be seen: the losses occur every day at the same time, and no further losses occur overnight.

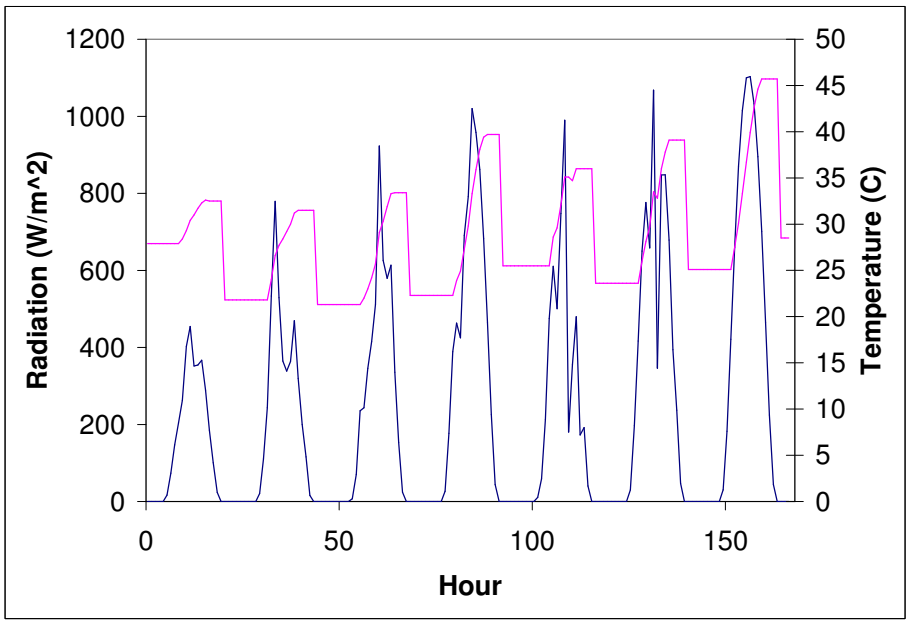

Fig. 5.2: Model output for this week in May tracks the tank water temperature and the radiation input.

5.3 Collector tilt and orientation

The annual energy collected (5.33kWh/day average) at the actual collector tilt at the residence in Santa Cruz, 18°, is within 3% of the energy produced at the optimal collector tilt, 35° (Figure 5.3). Variations in tilt of 25° lead to decreases in energy production of less than 8%. For a wide range of roof pitch, the most economical choice is very likely simply mounting the collector at the existing roof slope.

Energy production is also relatively insensitive to collector orientation (Figure 5.4). The energy collected is essentially equivalent for orientations from due South to 15° West of South. At 30° West of South, the decrease is 1.3%; at 45% it is 3.4%. With the collector

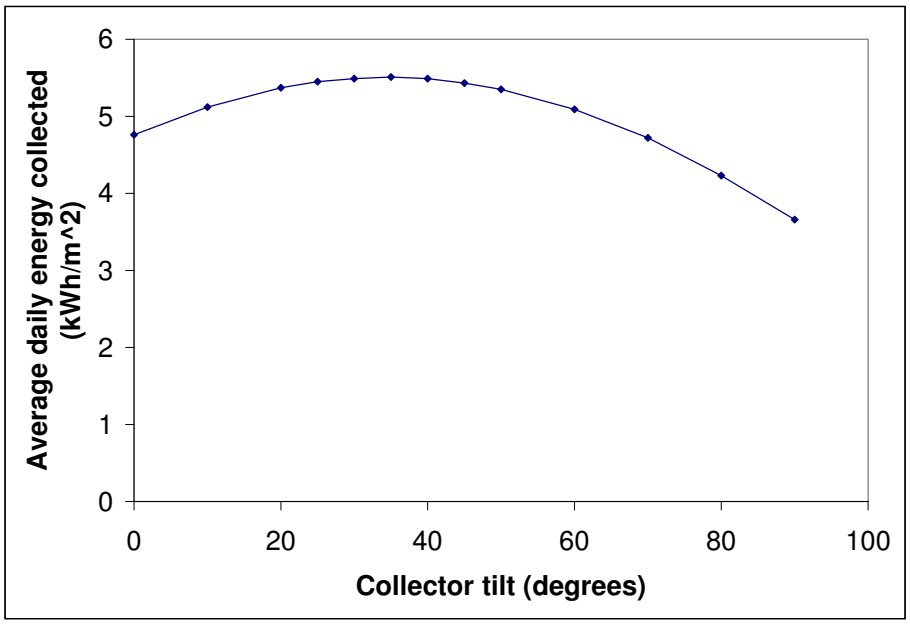

Fig. 5.3: Energy produced by the solar collector is maximized at a tilt of 35°.

oriented due west, energy production is lower by 13% than the optimal. Orientations to the east are slightly less favorable, presumably reflecting the influence of morning cloud cover. Again, for a wide range of roof orientations, the most economical choice is probably to mount the collectors with the same orientation as the roof.

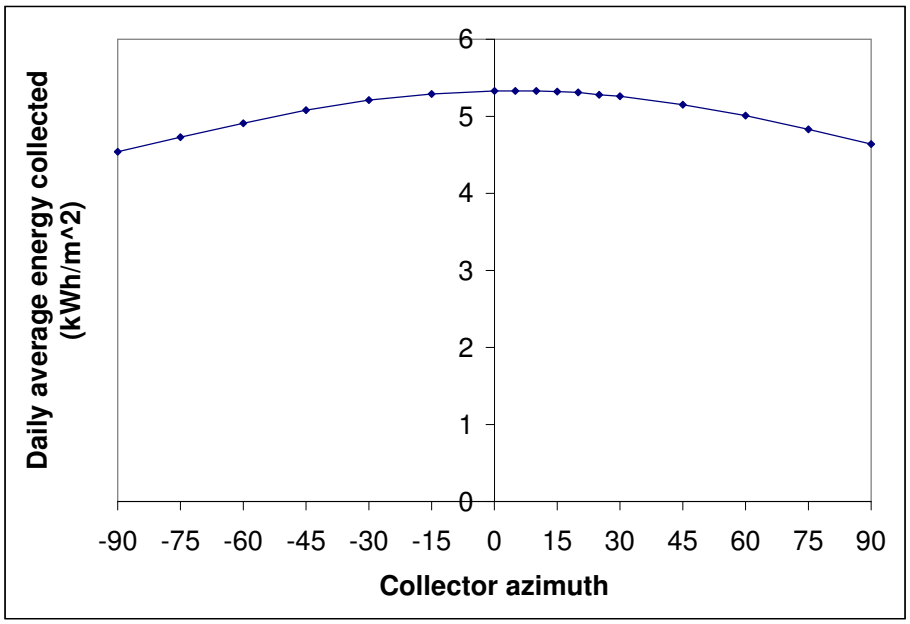

Fig. 5.4: Energy produced by the collector is insensitive to azimuth angle, with peak production occurring with orientation to the south and slightly west of south.

5.4 Collector area

Increasing collector area has diminishing returns in meeting annual hot water demand (Figure 5.5). Above a collector area of 5 m^2 (54 $ft.^2$), returns noticeably decrease. Meeting 90% of the annual heating load would require more than three 4ft.×10ft. collectors. This model result demonstrates the near-impossibility of heating water with the sun on cold cloudy days. The most cost-effective collectors are the first ones installed.

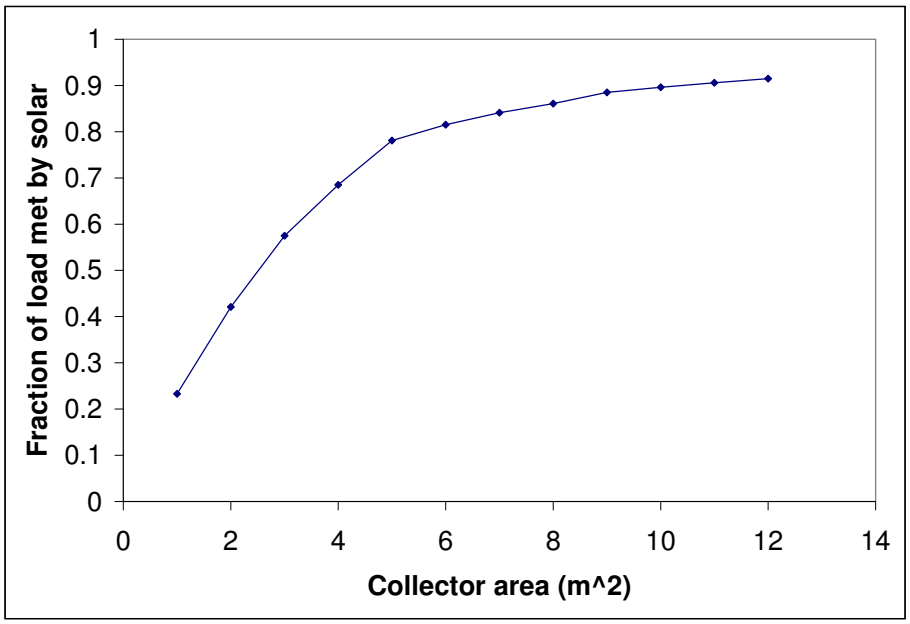

Fig. 5.5: Increasing collector area has diminishing returns in meeting the water heating demand.

5.5 Flow rate

The collector fluid flow rate determined here was 1.7 gal/min., or 0.106 kg/s. The flow rate used during collector rating was 0.055 kg/s. The flow rate was varied, and its effect determined on the fraction of annual heating provided. The effects of flow rate on collector performance are determined by Equations 18 – 20. According to these results, if the current flow rate were cut in half, the fraction of annual water heating provided would increase from 66% to 76%. The flow rate could be decreased by partially closing an inline valve. This is a promising path to pursue to increase the efficiency of the system.

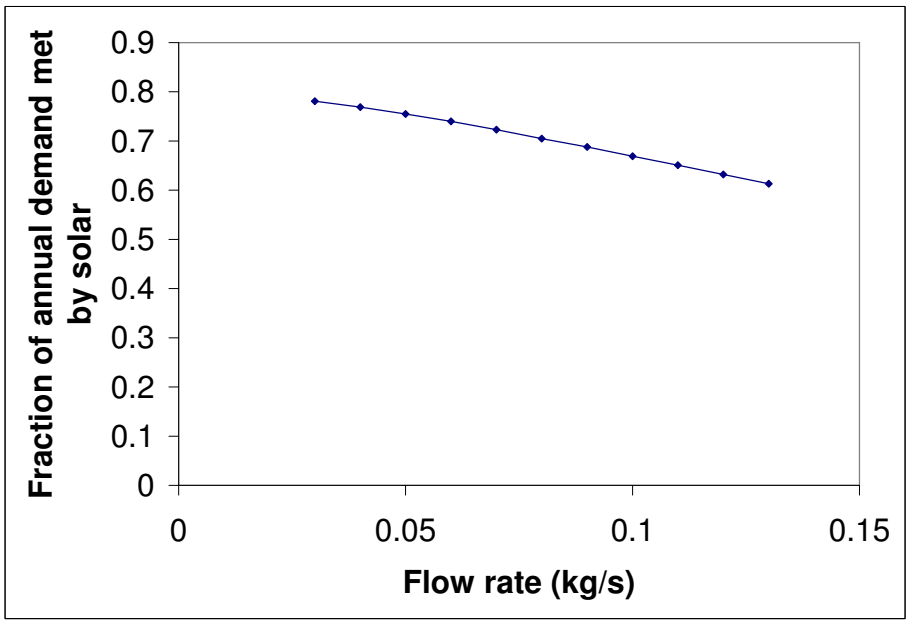

Fig. 5.6: Halving the flow rate from the existing 0.106kg/s to 0.05kg/s would increase the energy provided by the sun by 15%.

5.6 Economic analysis

No configuration of solar water heating system was cost-effective compared with a 70% efficient natural gas water heater. Table 5.3 shows the life cycle savings associated with ten collector configurations. Life cycle savings are defined to be the net present value (NPV) of heating water with solar energy and natural gas backup minus the cost of heating water with natural gas alone. Negative savings indicate that the solar heating does not pay for itself. The most cost-effective of the configurations modeled is the existing single black paint 4ft.×10ft collector. Adding a second collector lowers the overall initial cost per unit of energy collected. However, this lower unit cost is not enough to compensate for the diminishing

returns of additional collector surface. Current federal tax credits of 30%, up to $2000, obviously improve the economics. Changing the collector surface to the selective surface with a single 4ft.×10ft. chrome surface collector meets 71% of the annual load. However, this improved performance never balances its higher initial cost. The most cost-effective chrome surface collector configuration is a single 4ft.×8ft. collector.

Table 5.3: Net savings (losses) over a 30-year lifespan are lowest with one 4ft.×10ft. black painted surface collector.

Configuration	$32ft.^2$	$40ft.^2$	$64ft.^2$	$72ft.^2$	$80ft.^2$
Black paint surface	($4126)	($4081)	($5506)	($5617)	($6344)
Black paint surface + 30% tax credit	($2399)	($2293)	($3339)	($3450)	($4177)
Black chrome surface	($4198)	($4348)	($5784)	($6089)	($7015)
Black chrome surface + 30% tax credit	($2409)	($2440)	($3617)	($3922)	($4848)

These economic conclusions have assumed an escalation rate in the price of natural gas of 2% per year. If gas prices were to increase at a higher rate, the economics of solar heating would become more attractive (Table 5.4). However, the escalation rate would need to be 10% per year for the single 4ft.×10ft. collector system to have a positive 30-year life cycle savings.

Table 5.4: Changes in the assumed rate of escalation in natural gas prices strongly affect the life cycle savings of the solar water heating system.

Escalation rate	2%	4%	6%	8%	10%
Life cycle savings	($4084)	($3495)	($2092)	($1419)	$385

6 Conclusions

The existing solar water heating system at the residence in Santa Cruz was found by the model developed here to provide 66% of the annual water heating load. Increasing the

collector tilt to the optimal value (35°) increases the energy collected by less than 3%. The current orientation (due South) is optimal; a collector oriented Southwest would collect 3.4% less energy. A selective-surface collector would increased the fraction of energy provided to 71%, while also increasing the life-cycle losses by 7%. Cutting the collector fluid flow rate in half could potentially increase the solar fraction from 66% to 76%.

No configuration of solar water heating system was found which was as cost-effective over a 30-year period as a 70% natural gas water heater. The current configuration, with one 4ft.×10ft. collector, and an 80-gallon storage tank, was found to be the most cost-effective hypothetical option, with a 30-year net positive savings of -$4084.

The model could be improved by incorporating losses from the storage tank and piping, by modeling thermal stratification within the tank, by changing the assumed demand from a static once-per-day load to a more realistic demand profile, and by examining the effects of a stochastic radiation input.

References

Badescu, V. (2005). "Simulation analysis for the active solar heating system of a passive house." *Applied Thermal Engineering*, 25, 2754–2763.

Badescu, V. and Staicovici, M. (2006). "Renewable energy for passive house heating Model of the active solar heating system." *Energy and Buildings*, 38, 129–141.

Biaou, A. and Bernier, M. (2007). "Achieving total domestic hot water production with renewable energy." *Building and Environment*.

Bickford, C. (2007). "Sizing solar hot water systems." *Home Power*, April/May.

Bojic, M., Kalogirou, S., and Petronijevic, K. (2002). "Simulation of a solar domestic water heating system using a time marching model." *Renewable Energy*, 27, 441–452.

Bush, G. and Richards, L. (1980). *Solar Geometry and Time*, 239–267. Marcel Dekker, Inc.

Crowe, C., Elger, D., and Roberson, J. (2005). *Engineering Fluid Mechanics*. John Wiley & Sons, Inc.

DOE (2006). "Solar collectors." *U.S. Department of Energy*, http://www1.eere.energy.gov/solar/sh-basics-collectors.html.

DOE (2007). "Heat your water with the sun." *U.S. Department of Energy*, http://www.nrel.gov/docs/fy04osti/34279.pdf.

Duffie, J. and Beckman, W. (2006). *Solar Engineering of Thermal Processes*. John Wiley & Sons, Inc.

Gueymard, C. (2003). "Direct solar transmittance and irradiance predictions with broadband models. Part I: detailed theoretical performance assessment." *Solar Energy*, 74.

Hou, H., Wang, Z., Wang, R., and Wang, P. (2005). "A new method for the measurement of solar collector time constant." *Renewable Energy*, 30, 855–865.

I.E.A. (2004). "Worldwide capacity of solar thermal energy greatly underestimated." http://iea-shc.org/.

Kalogirou, S. (2004). "Solar thermal collectors and applications." *Progress in Energy and Combustion Science*, 30, 231–295.

Kazeminejad, H. (2002). "Numerical analysis of two dimensional parallel flow flat-plat solar collector." *Renewable Energy*, 26, 309–323.

Kleinbach, E., Beckman, W., and Klein, S. (1993). "Performance study of one-dimensional models for stratified thermal storage tanks." *Solar Energy*, 50, 155–166.

Li, Z. and Sumathy, K. (2002). "Performance study of a partitioned thermally stratified storage tank in a solar powered absorption air conditioning system." *Applied Thermal Engineering*, 22, 1207–1216.

Lima, J., Prado, R., and Taborianski, V. (2006). "Optimization of tank and flat-plate collector of solar water heting system for single-family households to assure economic efficiency through trnsys program." *Renewable Energy*, 31, 1581–1595.

Marion, W. and George, R. (2001). "Calculation of solar radiation using a methodology with worldwide potential." *Solar Energy*, 71, 275–283.

Marion, W. and Urban, K. (1995). *User's Manual for TMY2s*. National Renewable Energy Laboratory.

Marshall, R. (1999). "A generalised steady state collector model including pipe losses, heat exchangers, and pump powers." *Solar Energy*, 66, 469–477.

Maxwell, E. (1998). "METSTAT – The solar radiation model used in the production of the National Solar Radiation Data Base (NSRDB)." *Solar Energy*, 62, 263–279.

Muneer, T. and Gul, M. (2000). "Evaluation of sunshine and cloud cover based models for generating solar radiation data." *Energy Conversion and Management*, 41.

NREL (2007). "Solar water heating." *National Renewable Energy Laboratory*, www.nrel.gov/femp/ppt/solwater.ppt.

NSRDB (2007). "NSRDB hourly data files." *http://rredc.nrel.gov/solar/old-data/nsrdb/hourly/.*

Oliveski, R., Krenzinger, A., and Vielmo, H. (2003). "Comparison between models for the simulation of hot water storage tanks." *Solar Energy*, 75, 121–134.

Onur, N. (1993). "Forced convection heat transfer from a flat-plate model collector on roof of a model house." *Heat and Mass Transfer*, 28, 141–145.

Petkovsek, Z. and Rakovec, J. (1983). "The influence of meteorological parameters on flat-plate solar energy collector." *Archives for Meteorology, Geophysics, and Bioclimatolgy*, 33, 19–30.

PG&E (2007). "Natural gas watch." *http://www.pge.com/news/news-releases/q1_2007/070201.html.*

Pillai, I. and Banerjee, R. (2007). "Methodology for estimation of potential for solar water heating in a target area." *Solar Energy*, 81, 162–172.

RadiantHeatProducts (2007). "Superstor ultra indirect hot water heater." *http://www.radiantheatproducts.com/index.asp?category=9716.*

Sandia_National_Laboratory (2002). "Life cycle costing." *http://sandia.gov/pv/docs/LCcost.htm.*

Solarskies (2007). "Radco products." *http://solarskies.com/products/category-browse-subcategory?usca_p=t&category_id=3&subcategory_id=1&subsubcategory_id=0&how_many=20&start_rou*

SRCC (2007). "Summary of SRCC certified solar collector and water heating systems." *Solar Rating and Certification Corporation, http://solar-rating.org/SUMMARY/Dirsum_20070313.pdf.*

Weiss, W., Bergmann, I., and Faninger, G. (2005). "Solar heating worldwide." *Institue for Sustainable Technologies*, http://iea-shc.org/welcome/IEASHCSolarHeatingWorldwide2005.pdf.